12th International Symposium on Turbulence and Shear Flow Phenomena (TSFP12)
Osaka, Japan (Online), July 19-22, 2022

THE EFFECT OF LARGE EDDY BREAK-UP DEVICE ON ROUGH WALL TURBULENT BOUNDARY LAYER

Shubham Kumbhar
Department of Mechanical Engineering
University of Newcastle
University Dr, Callaghan NSW 2308
shubhambharat.kumbhar@uon.edu.au

Lyazid Djenidi
Department of Mechanical Engineering
University of Newcastle
University Dr, Callaghan NSW 2308
lyazid.djenidi@newcastle.edu.au

Farzin Ghanadi
Department of Mechanical Engineering
University of Newcastle
University Dr, Callaghan NSW 2308
farzin.ghanadi@newcastle.edu.au

Md Kamruzzaman
Department of Mechanical Engineering
University of Newcastle
University Dr, Callaghan NSW 2308
md.kamruzzaman@uon.edu.au

ABSTRACT

The effect of large eddy break up (LEBU) device on the rough wall turbulent boundary layer up to $Re_\theta \approx 12000$ is investigated using hot-wire anemometry. The pressure measurements (around a circular roughness element) are carried out to determine skin-friction coefficient (c_f) and friction velocity (U_τ). The LEBU is flat plate, installed at wall normal distance of 0.8δ (local boundary layer thickness) from the wall. The LEBU effect is observed immediate downstream of the device, where it creates a region of recirculating wake. At $43.7L_B$ (L_B is the LEBU chord length), maximum LEBU effect is reflected in the reduction in turbulence intensity. The boundary layer recovers around $50.4L_B$.

INTRODUCTION

The large eddies present in the outer layer of the turbulent boundary layer can be manipulated using the Large-Eddy Break-Up (LEBU) or Outer Layer Devices (OLD). These devices are known to reduce friction and induce total net drag on a smooth wall (Sahlin *et al.*, 1988). There is no study to understand how these devices disturb the rough wall turbulent boundary layer. The earlier outer layer manipulation studies by Yajnik & Acharya (1978) and Hefner *et al.* (1980) expressing the capability of the thin plate device to reduce the friction drag provided a breeding ground for the number of LEBU studies worldwide. Corke *et al.* (1981, 1982) reported a reduction in the turbulence intensity up to 100δ (boundary layer thickness) and serious net drag reduction (up to 20%) with tandem LEBU arrangement. In the follow up study by Anders & Watson (1985), the net drag reduction up to 7% was recorded. The LEBU popularity dropped significantly after the towing tank experiments carried out by Sahlin *et al.* (1988) proving the incapability of the LEBU to reduce net drag owing to the device drag added by LEBU itself.

The LEBU devices studies continued even after several failed attempts of using LEBU for net drag reduction. In recent years the advancement of computer resources has brought a new wave of numerical studies focussing more on understanding the LEBU effects (Kim *et al.*, 2017; Chin *et al.*, 2017; Chan *et al.*, 2021). It can be said that a fair amount of work has been dedicated to exploring the application of these devices on a smooth wall. Comparatively much less attention was given to the LEBU effects on the rough wall. Bandyopadhyay (1986) found that the outer layer devices are less effective for drag reduction in rough walls as compared to the smooth wall. But no literature is found which depicts the interest to learn the detailed effect of these so-called 'drag enhancing' devices (of course, when looked at from a drag reduction perspective) on the structure of rough wall turbulent boundary layer. The primary aim of the present study is to fill the critical knowledge gap in the area of wall turbulence, by investigating how a fully developed turbulent boundary layer responds to LEBU placed in the rough wall turbulent boundary layer. The results are also compared with no LEBU results.

EXPERIMENTAL SETUP

The open-return blower type wind tunnel at the university of Newcastle is used for these experiments which was previously used by Kamruzzaman *et al.* (2015) to investigate the drag of turbulent boundary layer with transverse circular rods. The 5.4 m long test section is 0.15 m wide and 0.9 m high cross-section. The zero-pressure gradient is maintained in the entire working section of the wind tunnel by adjusting the one side wall to compensate for the growth of the boundary layer. The boundary layer is tripped at the contraction by a 4 mm diameter rod followed by 170 mm long strip of No. 40 grit sandpaper. Antonia *et al.* (1990) confirmed the behaviour of the turbulent boundary layer (tripped by using a rod and sandpaper) to be similar as the fully developed turbulent boundary layer. The rough wall consisted of the copper-coated circular rods placed equidistant over the entire width of the working section (see figure 1). The diameter of the circular rods is 1.6 mm, and the ratio is set to be $\lambda/k = 16$. According to Leonardi *et al.* (2003) for $\lambda/k = 16$ the viscous drag is very small, and the form drag can be closely approximated to the total drag. The virtual origin (d_0) is determined by using the method introduced by Jackson (1981) who measured d_0 from base of roughness with the distance to the centroid of the moment of

the forces acting on rod roughness. This technique was used by (Kamruzzaman *et al.*, 2015; Talluru *et al.*, 2016; Djenidi *et al.*, 2017). In this case, $d_0/k = 0.48$, d_0 is determined by estimating the centroid of forces acting on roughness elements from the pressure distribution around the roughness element.

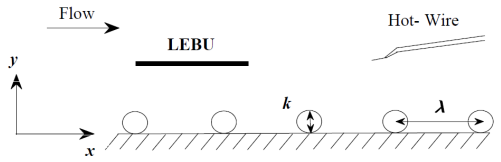

Figure 1. A schematic of the experimental setup. The origin of x is taken at the leading edge of the rough wall.

Hot-wire anemometry is used for streamwise velocity measurements. The Dantec 55P15 single hot-wire probe, has spacing of 1.5 mm with 2.5 μm Wollaston Pt wire soldered between two prongs. In house built constant temperature anemometer (CTA) circuit is used to operate hot-wire at an overheat ratio of 1.5. The signal from the CTA is amplified, offset and low- pass filtered at cut-off frequency (fc) of 12000 Hz with sampling frequency set at $2fc$. The positioning of the hot-wire probe close to the wall is accomplished using Celestron digital microscope (resolution = 1 micron) mounted on fine threaded traversing system. The dial indicator with the divisions of 0.001 m is set at zero when the microscope is focussed at the wall, the displacement is measured as the microscope focus is shifted from wall to probe. The Mitutoyo height gauge (resolution = 0.01 mm) is used for 32 points measurements (spaced logarithmically) between 0.5 mm to 89.4 mm. The temperature fluctuation is measured for the entire duration of the experiment using BAT-10 thermocouple (resolution = 0.1° C). At the beginning and end of every experiment the hot-wire is calibrated against the pitot tube (fixed) immersed in the undisturbed free stream flow. To counter the hot-wire voltage drift the linear interpolation is used between the pre and post calibration data.

The friction velocity ($U_\tau = \sqrt{\tau_w/\rho}$, where, τ_w is the wall shear stress and ρ is the density of the fluid) is obtained by measuring the pressure distribution around the rod and defect chart method (both methods give consistent values of U_τ within 2%). The pressure measurement is carried out at x = 2.54 m (origin of x is taken at the leading edge of the rough wall). At this location the circular rod is replaced by non-coated hollow steel cylinder. A hole of 0.32 mm diameter is drilled through the wall of cylinder, it is connected to the Furnace Control FC 0332 micromanometer (Range: $0-50Pa$, Accuracy: $0.0125Pa$, 0.025% full scale output). The cylinder is rotated by 10°(with minimum step angle resolution of 1.8) from 0° - 360° with more than 60 seconds measurements at each rotation. The 600 mm long LEBU is made of the Aluminium with 1 mm of thickness and 60 mm chord length to occupy the tunnel's entire span width. The 'pin-and-strut' configuration is used to hold the position of LEBU at x = 2.49 m (fully developed region). This LEBU mechanism is designed to perform effective wall-normal distance study as well as check the effects of the device at different locations. For the present study, the LEBU is placed at the wall-normal distance of 0.8δ because this location is proven to be effective to disturb the boundary layer in various studies for example (Corke *et al.*, 1982; Anders & Watson, 1985). The present study is conducted at free stream velocity of U_∞ = 8 m/s and 12 m/s, while the momentum thickness Reynolds numbers Re_θ ranging from 7004 to 11985 with U_τ = 0.48 at 8 m/s and U_τ = 0.75 at 12 m/s.

RESULTS AND DISCUSSION

Pressure Measurements

Figure 2(a) & (b) describes the pressure distribution around a roughness element for U_∞ = 8 m/s and 12 m/s at different x/L_B (L_B is the LEBU chord length). The measurements were taken at two different regions, close to the tunnel inlet and further away (fully developed region). These distributions are used to calculate the (c_f) as follows.

$$c_f = \frac{2F_D}{\rho U_\infty^2 k}$$

where, pressure drag (F_D) is,

$$F_D = \int_0^{2\pi} \tfrac{1}{2} P_s \, k cos\alpha \, d\alpha$$

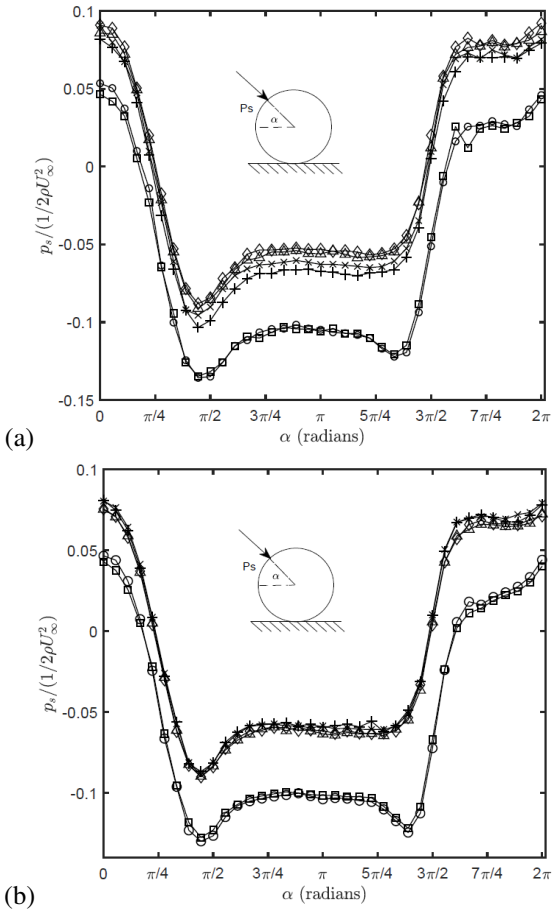

Figure 2. Distribution of the normalised static pressure around a rod at different free stream velocities. (a) U_∞ = 8 m/s (b) U_∞ = 12 m/s. Symbols, ○: $17.4L_B$, □: $20.6L_B$, +: $40.8L_B$, ×: $43.0L_B$, △: $45.8L_B$, ◇: $48.2L_B$.

The streamwise variation of c_f for U_∞ = 8 m/s and 12 m/s are shown in the figure 3. We found that c_f is constant in the range of 40 to 50 for U_∞ = 8 m/s. For U_∞ = 12 m/s the value of c_f is increasing with x/L_B. The change in magnitude of c_f for different velocities reflects a Reynolds number effect.

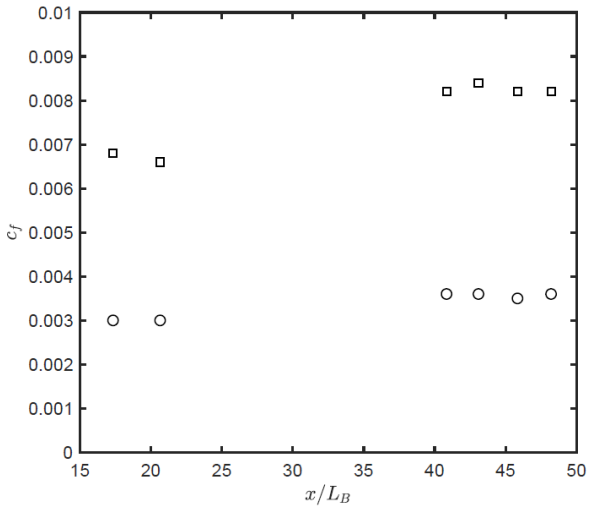

Figure 3. Variation in C_f with x/L_B for λ/k = 16. Symbols □: LEBU, U_∞ = 12 m/s, ○: LEBU, U_∞ = 8 m/s.

Mean Velocity and Velocity Defect

The mean velocity profiles at seven streamwise locations are presented in the figure 4 . As suggested by Kamruzzaman *et al.* (2015) U_τ and δ is used as scaling parameters due to their better scalability for rough wall. The No LEBU rough wall data is used for the purpose of comparison.

Table 1. Boundary layer properties at different streamwise locations (Hot-wire measurements). Here, NLB: No LEBU.

x (m)	*Symbol*	U_∞ (m/s)	δ (m)	δ^* (m)	θ (m)	Re_τ	Re_θ
NLB	●	8	0.083	0.021	0.012	2873	6548
42.4L_B	□	8	0.084	0.022	0.013	2641	7286
43.7L_B	○	8	0.083	0.021	0.013	2663	7277
45.0L_B	+	8	0.085	0.021	0.013	2678	7004
46.4L_B	*	8	0.086	0.023	0.013	2756	7527
47.7L_B	×	8	0.087	0.024	0.014	2845	7615
49.0L_B	◇	8	0.087	0.024	0.014	2839	7757
50.4L_B	▽	8	0.087	0.023	0.013	2827	7410
NLB	●	12	0.083	0.020	0.012	4151	9710
42.4L_B	□	12	0.086	0.022	0.013	4049	11072
43.7L_B	○	12	0.084	0.021	0.013	3968	10625
45.0L_B	+	12	0.087	0.023	0.013	4398	11985
46.4L_B	*	12	0.087	0.025	0.014	4304	11886
47.7L_B	×	12	0.087	0.024	0.014	4358	11663
49.0L_B	◇	12	0.087	0.024	0.014	4360	11769
50.4L_B	▽	12	0.086	0.023	0.013	4240	11025

Figure 4(a) & (b) shows the mean velocity profiles for U_∞ = 8 m/s and 12 m/s respectively. It appears that LEBU disturbs the boundary layer significantly. The inner layer comparison of LEBU and No LEBU profiles show significant deviation from each other. Immediately downstream of the LEBU, 42.4L_B there is very strong region of recirculating wake ($y/\delta \sim 0.8$). Also, the inner layer is affected the most by LEBU ($y/\delta \leq 0.04$) at 43.7L_B.

Figure 4(c) & (d) presents the mean velocity profiles over rough wall (with and without LEBU) in the velocity defect form ($(U_\infty - U)/U_\tau$ vs y/δ). These profiles show a good collapse reflecting that seen in figure (a) & (b). The wake due to the LEBU device is also observed clearly in velocity defect form around $y/\delta \sim 0.8$. The turbulence intensity profiles are presented in the Figure 4(e) & (f). At 43.7L_B the turbulence intensity is reduced. For $Re_\theta \geq 11072$ this gap seems to have closed by small amount which means for higher Re_θ, the LEBU effect is reduced. The LEBU effect seems to have vanished from the outer layer at 50.4L_B. It would be interesting to compare these results with smooth wall to understand the recovery of boundary layer on different surfaces.

CONCLUSIONS

The hot-wire anemometry measurements are carried out on the rough wall turbulent boundary layer subjected to the LEBU device. The pressure distribution around a roughness element is measured to determine c_f and U_τ. The c_f variation for different velocities reflects the Reynolds number effect. The mean velocity profiles at seven streamwise locations are presented. The inner layer comparison of LEBU and No LEBU profiles show significant deviation from each other. Immediately downstream of the LEBU, 42.4L_B there is very strong region of recirculating wake ($y/\delta \sim 0.8$). The inner layer is affected the most by LEBU (y/ 0.04) at 43.7LB. This device also acts to reduce the turbulence intensity (at 43.7L_B). The boundary layer recovers around 50.4L_B as the LEBU effect (wake) from the outer layer disappears.

Acknowledgments

The Australian Research Council (ARC) is gratefully acknowledged for the financial support of this work.

REFERENCES

Anders, J & Watson, R 1985 Airfoil large-eddy breakup devices for turbulent drag reduction. In *Shear Flow Control Conference*, p. 520.

Antonia, RA, Bisset, DK & Browne, LWB 1990 Effect of reynolds number on the topology of the organized motion in a turbulent boundary layer. *J. Fluid Mech.* **213**, 267–286.

Bandyopadhyay, PR 1986 Drag reducing outer-layer devices in rough wall turbulent boundary layers. *Exp. Fluids* **4** (5), 247–256.

Chan, IC, Örlü, Ramis, Schlatter, Philipp & Chin, RC 2021 The skin-friction coefficient of a turbulent boundary layer modified by a large-eddy break-up device. *Phys. Fluids* **33** (3), 035153.

Chin, Cheng, Örlü, Ramis, Monty, Jason, Hutchins, Nicholas, Ooi, Andrew & Schlatter, Philipp 2017 Simulation of a large-eddy-break-up device (lebu) in a moderate reynolds number turbulent boundary layer. *Flow T. Comb.* **98** (2), 445–460.

Corke, TC, Nagib, HM & Guezennec, YG 1982 A new view

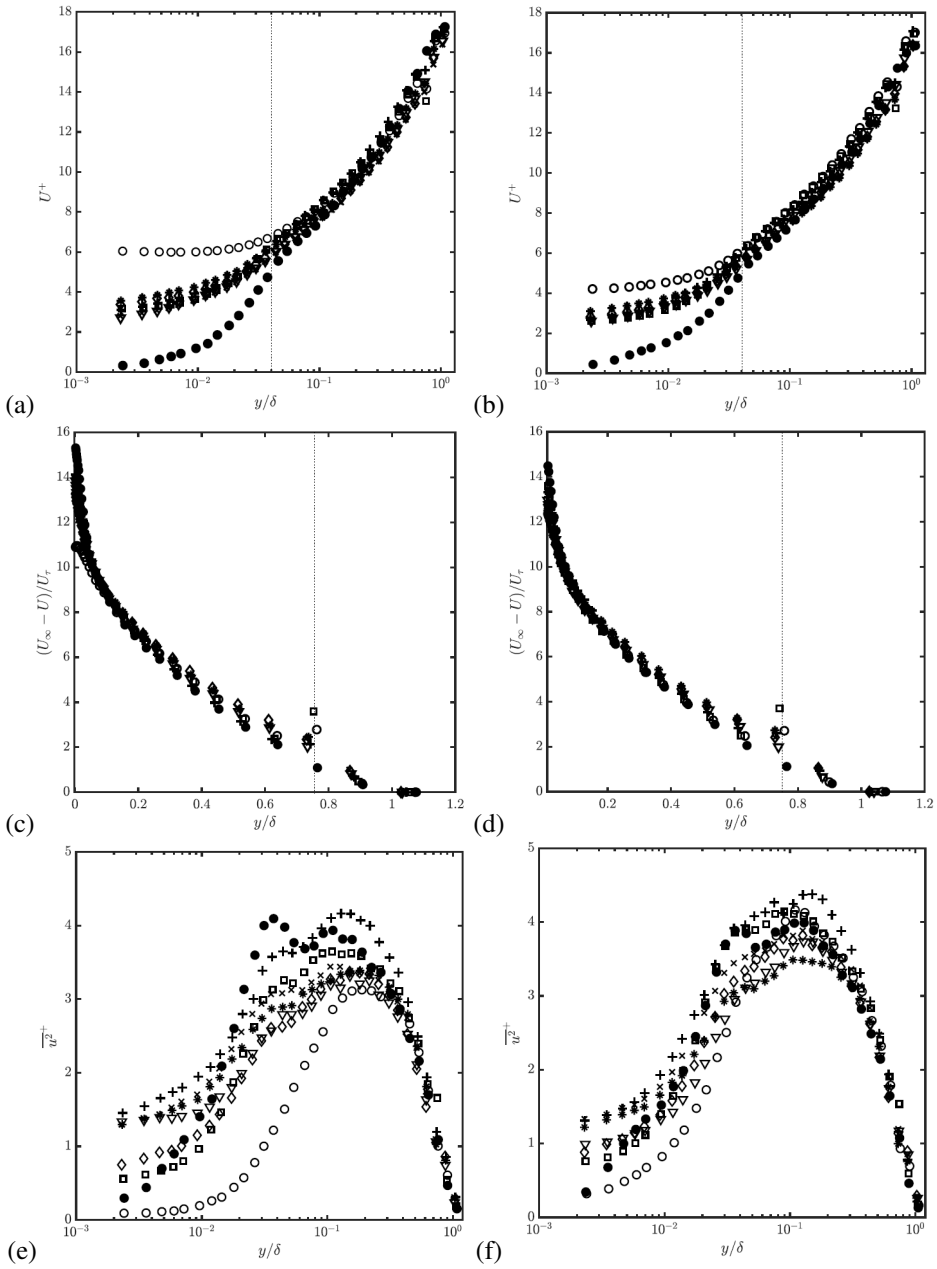

Figure 4. Comparison of a mean velocity, velocity defect, and turbulence intensity profiles between the 8 m/s and 12 m/s data (see table 1 for symbols).

on origin, role and manipulation of large scales in turbulent boundary layers. *Tech. Rep.*.

Corke, Thomas C, Guezennec, Y & Nagib, Hassan M 1981 Modification in drag of turbulent boundary layers resulting from manipulation of large-scale structures. *Tech. Rep.*. NASA.

Djenidi, L, Lefeuvre, N, Kamruzzaman, MD & Antonia, RA 2017 On the normalized dissipation parameter in decaying turbulence. *J. Fluid Mech* **817**, 61–79.

Hefner, Jerry N, Weinstein, Leonard M & Bushnell, Dennis M 1980 Large-eddy breakup scheme for turbulent viscous drag reduction. In *Symposium on Viscous flow drag reduction*.

Jackson, PS 1981 On the displacement height in the logarithmic velocity profile. *J. Fluid Mech* **111**, 15–25.

Kamruzzaman, Md, Djenidi, L, Antonia, RA & Talluru, KM 2015 Drag of a turbulent boundary layer with transverse 2d circular rods on the wall. *Exp. Fluids* **56** (6), 1–8.

Kim, Joon-Seok, Hwang, Jinyul, Yoon, Min, Ahn, Junsun & Sung, Hyung Jin 2017 Influence of a large-eddy breakup device on the frictional drag in a turbulent boundary layer. *Phys. Fluids* **29** (6), 065103.

Leonardi, S, Orlandi, Paolo, Smalley, RJ, Djenidi, L & Antonia, RA 2003 Direct numerical simulations of turbulent channel flow with transverse square bars on one wall. *J. Fluid Mech* **491**, 229–238.

Sahlin, Alexander, Johansson, Arne V & Alfredsson, P Henrik 1988 The possibility of drag reduction by outer layer manipulators in turbulent boundary layers. *Phys. Fluids* **31** (10), 2814–2820.

Talluru, KM, Djenidi, L, Kamruzzaman, Md & Antonia, RA 2016 Self-preservation in a zero pressure gradient rough-wall turbulent boundary layer. *J. Fluid Mech* **788**, 57–69.

Yajnik, KS & Acharya, M 1978 Non-equilibrium effects in a turbulent boundary layer due to the destruction of large eddies. In *Struc. Mech. Turbulence I*, pp. 249–260. Springer.